Electromagnetic scattering by spherical negative-refractive-index particles: Low-frequency resonance and localization parameters

Zheng Liu,[1] Zhifang Lin,[2] and S. T. Chui[2]

[1]*Surface Physics Laboratory and Research Center of Theoretical Physics, Fudan University, Shanghai 200433, China*
[2]*Bartol Research Institute, University of Delaware, Newark, Delaware 19716, USA*

The Mie scattering of electromagnetic waves of wave vector k by spherical negative-refractive-index particles of radius a exhibits an unusual resonance at $ka \to 0$. The scattering enhancement from the $ka \to 0$ resonance is insensitive to the size of scatterers, distinct from the Mie scattering resonances from positive-refractive-index particles. For media consisting of a collection of the negative-refractive-index particles, the unusual resonance results in a significant reduction of the localization parameter, providing a possibility to reach the light localization transition by reducing the wave vector k, in analogy to electronic systems.

I. INTRODUCTION

Much experimental and theoretical efforts has been recently devoted to the study of a new type of metamaterials that have simultaneously negative electric permittivity ϵ and magnetic permeability μ and are thus termed as negative-refractive-index materials (NIM's), or "left-handed materials" [1–14]. Over thirty years ago, Veselago [15] predicted theoretically that electromagnetic waves propagating in isotropic NIM's possess several peculiar characteristics, including anomalous refraction, reversal of both the Doppler shift and the Cerenkov radiation, and reversal of radiation pressure to radiation tension. Due to the absence of naturally occurring materials having both negative ϵ and negative μ, however, Veselago's prediction did not receive much attention until recently, when a system consisting an array of resonators and metallic wires was prepared and demonstrated to have negative refractive index, for electromagnetic waves propagated in some special direction and polarization in a narrow microwave frequency region [5–8]. The successful fabrication of NIM's aroused great interest in exploring their unusual electromagnetic effects that may lead to useful application. Among others, ideas have been proposed which use NIM's to achieve subwavelength focusing [4,10], to open an unconventional photonic band gap [9], and to enhance photon tunneling [16,17].

Concurrently, there has been an ongoing interest in the field of multiple electromagnetic scattering and transport of light in disordered media. This is initially motivated by the fact that many electronic effects have their analog in electromagnetic scattering systems [18–28]. Among these are the coherent backscattering effect, which is the optical counterpart of electronic weak localization [18–20], the photonic Hall effect [24], the anisotropic light diffusion [25], and, in particular, the localization of light [22,26,27]. To achieve localization, the localization parameter $\eta = k l_t$ needs to be reduced, where $k = 2\pi/\lambda$ is the light wave vector with λ the wavelength, and $l_t = l_s/(1-g)$ is the transport mean free path with $g = \langle \cos\theta \rangle$ denoting the asymmetry parameter [29,30]. The scattering mean free path l_s is given, in first approximation, by $l_s = 1/\rho\sigma_s$ with ρ the number density of

scatterers and σ_s the total scattering cross section. The Mie scattering cross section σ_s depends on the magnetic permeability μ_s, the electric permittivity ϵ_s, as well as the size of the scatterers. Let f_v and a denote, respectively, the volume fraction and radius of the scatterers, and Q_s be the efficiency for scattering, the localization parameter η can be written as

$$\eta = \frac{4}{3f_v} \frac{x}{Q_s(1-g)}, \tag{1}$$

where $x = ka$ is the size parameter. In general

$$Q_s \sim \frac{1}{x^2} \tag{2}$$

at resonance points [30], one may intuitively hope to minimize the localization parameter and reach the localization transition ($\eta \sim 1$) by reducing k or $x = ka$, as in electronic systems. However, for ordinary materials with positive ϵ and μ, hereinafter referred to as positive-refractive-index materials (PIM's), resonance usually occurs only in the intermediate frequency regime ($x \sim 1$) or large particle limit ($x \gg 1$), while in the small-particle limit ($x \ll 1$), the Rayleigh law points out that Q_s is proportional to x^4, suggesting $\eta \propto 1/x^3$. As a result, a reduction of k will lead to an increase of the localization parameter, unfavorable to light localization. Localization of light is, up to now, believed possible only at an intermediate wavelength window, $\lambda \sim a$, where resonance arises such that the efficiency for scattering can be maximized. With the advent of NIM's, it is desirable to study if disordered system composed of NIM particles may help to decrease the localization parameter and approach the localization transition by inducing resonance in small-particle limit. In this paper, we report an investigation of light scattering and the localization parameter of light in the presence of NIM's. It is found that the NIM's may exhibit a unique type of resonance at $x \to 0$. The scattering enhancement in the small-particle limit due to the $x \to 0$ resonant effect is insensitive to the size of scatterers and results in a significant reduction of the localization parameter η, suggesting a pos-

sibility to induce the light localization transition by reducing the wave vector k, in analogy to electronic systems. We now describe our results in detail.

II. MIE SCATTERING BY NIM PARTICLES

Let us consider the scattering of light by a NIM particle [31]. The quantity of interest in single scattering is the efficiency for scattering Q_s. It can be expressed in terms of the Mie coefficients a_n and b_n [29,30] as

$$Q_s = \frac{2}{x^2} \sum_{n=1}^{\infty} (2n+1)(|a_n|^2 + |b_n|^2). \quad (3)$$

The Mie coefficients are given by

$$a_n = \frac{\mu_m m_s \psi_n(y) \psi_n'(x) - \mu_s \psi_n(x) \psi_n'(y)}{\mu_m m_s \psi_n(y) \xi_n'(x) - \mu_s \xi_n(x) \psi_n'(y)}, \quad (4)$$

$$b_n = \frac{\mu_s \psi_n(y) \psi_n'(x) - \mu_m m_s \psi_n(x) \psi_n'(y)}{\mu_s \psi_n(y) \xi_n'(x) - \mu_m m_s \xi_n(x) \psi_n'(y)}, \quad (5)$$

where $y = m_s x$, the relative refractive index $m_s = n_s/n_m$, with $n_s = \sqrt{\epsilon_s}\sqrt{\mu_s}$, ϵ_s, and μ_s ($n_m = \sqrt{\epsilon_m}\sqrt{\mu_m}$, ϵ_m and μ_m) are, respectively, the refractive index, electric permittivity, and magnetic permeability for the scatterer (surrounding medium). The Ricatti-Bessel functions ψ_n and ξ_n are defined in terms of the spherical Bessel functions of the first and third kinds, respectively, $\psi_n(x) = x j_n(x)$ and $\xi_n(x) = x h_n^{(1)}(x)$; the prime denotes differentiation with respect to the argument. To discuss resonance for a lossless sphere, it is convenient to introduce real phase angles [30] defined by

$$\tan \alpha_n = \frac{p_n^{(\alpha)}}{q_n^{(\alpha)}} = -\frac{\mu_m m_s \psi_n(y) \psi_n'(x) - \mu_s \psi_n(x) \psi_n'(y)}{\mu_m m_s \psi_n(y) \chi_n'(x) - \mu_s \chi_n(x) \psi_n'(y)}, \quad (6)$$

$$\tan \beta_n = \frac{p_n^{(\beta)}}{q_n^{(\beta)}} = -\frac{\mu_s \psi_n(y) \psi_n'(x) - \mu_m m \psi_n(x) \psi_n'(y)}{\mu_s \psi_n(y) \chi_n'(x) - \mu_m m \chi_n(x) \psi_n'(y)}, \quad (7)$$

with the Ricatti-Bessel function $\chi_n(x) = -x y_n(x)$ defined based on the spherical Bessel functions of the second kind $y_n(x)$. In terms of phase angles, the Mie coefficients a_n and b_n are given by

$$a_n = \frac{\tan \alpha_n}{\tan \alpha_n + i} = \frac{1}{2}(1 - e^{2i\alpha_n}), \quad (8)$$

$$b_n = \frac{\tan \beta_n}{\tan \beta_n + i} = \frac{1}{2}(1 - e^{2i\beta_n}), \quad (9)$$

and the efficiency for scattering Q_s reads [30]

$$Q_s = \frac{2}{x^2} \sum_{n=1}^{\infty} (2n+1)(\sin^2 \alpha_n + \sin^2 \beta_n). \quad (10)$$

The cases when α_n or β_n are $\pi/2$, $3\pi/2$ etc., namely, $\tan \alpha_n \to \infty$ or $\tan \beta_n \to \infty$, define the resonance points [30] at which Q_s shows a peak. It is also noted when $|\tan \alpha_n| \gg 1$ or $|\tan \beta_n| \gg 1$, corresponding to $\sin^2 \alpha_n \to 1$ or $\sin^2 \beta_n \to 1$, respectively, scattering can be greatly enhanced as well.

In the Rayleigh limit, with both $x \ll 1$ and $|m_s| x \ll 1$, we have

$$p_n^{(\alpha)} \sim (\epsilon - 1) x^{2n+1} + o(x^{2n+3}), \quad (11)$$

$$p_n^{(\beta)} \sim (\mu - 1) x^{2n+1} + o(x^{2n+3}), \quad (12)$$

$$q_n^{(\alpha)} = \left(\epsilon + \frac{n+1}{n} \right) + c_n^{(2)} x^2 + c_n^{(4)} x^4 + c_n^{(6)} x^6 + o(x^8), \quad (13)$$

$$q_n^{(\beta)} = \left(\mu + \frac{n+1}{n} \right) + d_n^{(2)} x^2 + d_n^{(4)} x^4 + d_n^{(6)} x^6 + o(x^8), \quad (14)$$

where the expansion coefficients $c_n^{(2)}$, $d_n^{(2)}$, $c_n^{(4)}$ and $d_n^{(4)}$ etc. depend on ϵ and μ, with $\epsilon = \epsilon_s/\epsilon_m$ and $\mu = \mu_s/\mu_m$. Hereinafter, without loss of generality, we assume $\epsilon_m = \mu_m = 1$ for simplicity. For $n = 1$, which represents the dipole contributions and is dominant in small-particle limit, the expansion coefficients for $q_1^{(\alpha)}$ are given by

$$c_1^{(2)} = 1 - \frac{\epsilon}{2} - \frac{2\epsilon\mu}{5} - \frac{\epsilon^2\mu}{10}, \quad (15)$$

$$c_1^{(4)} = -\frac{1}{4} + \frac{3\epsilon}{8} - \frac{\epsilon\mu}{5} + \frac{\epsilon^2\mu}{20} + \frac{\epsilon^2\mu^2}{140} + \frac{\epsilon^3\mu^2}{280}, \quad (16)$$

$$c_1^{(6)} = \frac{1}{72} - \frac{5\epsilon}{144} + \frac{\epsilon\mu}{20} - \frac{3\epsilon^2\mu}{80} + \frac{3\epsilon^2\mu^2}{280} - \frac{\epsilon^3\mu^2}{560} - \frac{\epsilon^3\mu^3}{1890}$$
$$- \frac{\epsilon^4\mu^3}{15120}, \quad (17)$$

while $d_1^{(2)}$, $d_1^{(4)}$, and $d_1^{(6)}$ are given by an interchange between μ and ϵ on $c_1^{(2)}$, $c_1^{(4)}$, and $c_1^{(6)}$, respectively. From Eqs. (11) to (14), it follows that for ordinary PIM's no resonance appears in the Rayleigh limit. The efficiency for scattering Q_s is thus governed by the Rayleigh law $Q_s \propto x^4$, excluding the possibility of reaching the localization transition by reducing k or x. However, for NIM, as ϵ and μ take negative values, the following resonance cases are found to arise at $x \to 0$, leading to new x dependence of Q_s different from the Rayleigh law: (1) electric (magnetic) dipole resonance for $\epsilon = -2$ and $\mu = -5$ ($\epsilon = -5$ and $\mu = -2$), giving rise to

$$Q_{sca} \sim \frac{6}{x^2}; \quad (18)$$

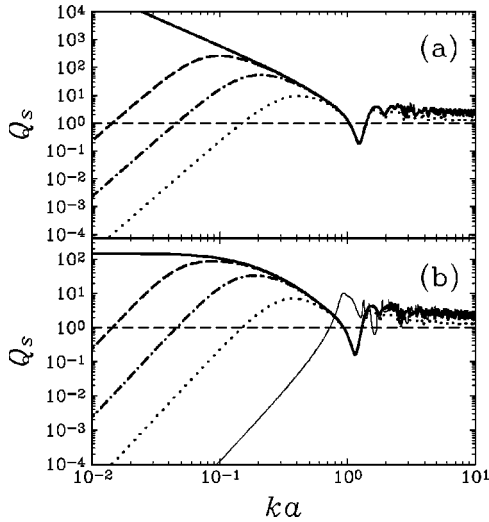(2) magnetic dipole resonance for $\mu = -2$ and $\epsilon \neq -5$, resulting in

FIG. 1. The efficiency for scattering Q_s vs size parameter ka for the cases with (a) $\epsilon = -5$, $\mu = -2 + i\delta$, and (b) $\epsilon = -6$, $\mu = -2 + i\delta$, where $\delta = 0$ (solid lines), 0.001 (dashed lines), 0.01 (dashed-dotted lines), and 0.1 (dotted lines). For comparison, Q_s vs ka for the case with $\epsilon = 6$ and $\mu = 2$, typical for ordinary PIM's is shown in (b) as thin solid line.

$$Q_{sca} \sim \frac{150}{(\epsilon+5)^2}; \tag{19}$$

(3) electric dipole resonance for $\epsilon = -2$ and $\mu \neq -5$, leading to

$$Q_{sca} \sim \frac{150}{(\mu+5)^2}; \tag{20}$$

(4) electric (magnetic) quadrupole resonance for $\epsilon = -3/2$ and $\mu = -7/3$ ($\epsilon = -7/3$ and $\mu = -3/2$), yielding

$$Q_{sca} \sim \frac{72}{5}. \tag{21}$$

To illustrate the $x \to 0$ resonance behavior, Q_s as a function of size parameter x is given in Fig. 1 for values of the susceptibility at the magnetic dipole resonance, namely, cases (1) and (2). The solid lines show the cases when there is no loss. The behavior $Q_s \sim 1/x^2$ and $Q_s \sim$ constant is clearly seen when $x < 1$ for cases (1) and (2), corresponding to Figs. 1(a) and 1(b), respectively. Q_s with varying amounts of loss added to the permeability μ that causes the magnetic dipole resonance at $x \to 0$ are also shown in Fig. 1. As x decreases, Q_s increases first, displaying the enhanced behavior near resonance, then due to loss Q_s decreases in proportion to x^4, recovering the Rayleigh law. For comparison, Q_s vs x is also shown in Fig. 1(b) for the case with $\epsilon = 6$ and $\mu = 2$, as an example for PIM scatterer. The maximum value of Q_s is seen to shift considerably to the low-frequency limit for NIM even if in some cases it may not be far greater than that for the PIM counterpart. The considerable increase of Q_s, as well as the shift of the maximum Q_s towards the
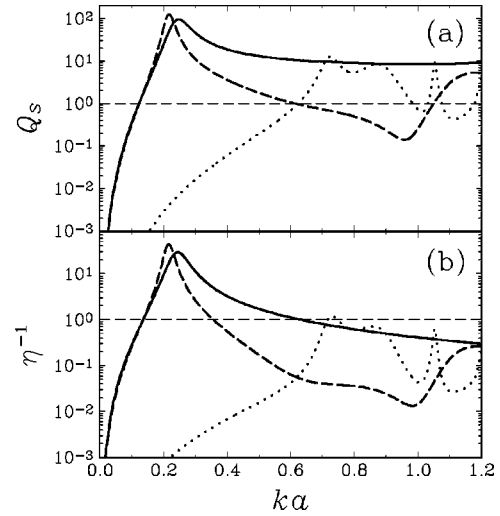

FIG. 2. The efficiency for scattering Q_s (a) and the inverse of the localization parameter η^{-1} (b) vs size parameter ka for the cases with $\epsilon = -2.1$, $\mu = -1$ (solid line), $\epsilon = -10$, $\mu = -1.9$ (dashed line), and $\epsilon = 10$, $\mu = 2$ (dotted line).

small x end, significantly reduces the localization parameter η, as will be demonstrated below.

The enhancement of Q_s in the small-particle limit for NIM can come from large values of $|\tan \alpha_n|$, $|\tan \beta_n|$ and is not limited to the resonance for particular values of ϵ and μ as in cases (1)–(4), but it also occurs when μ or ϵ is close to -2. For example, an increase of Q_s near the magnetic dipole resonance can be established as follows. For a given μ close to -2, $|\tan \beta_1|$ can be enhanced if $q_1^{(\beta)}$ is small. To achieve this we retain $q_1^{(\beta)}$ up to terms of order, say, x^6 as shown in Eq. (14), and find if the polynomial in terms of x possesses a root x_0 satisfying $0 < x_0 \ll 1$. If such a solution can be found it follows from Eq. (7) that $|\tan \beta_1| \sim 1/x_0^5 \gg 1$, resulting in a great enhancement of scattering near $x = x_0$. Indeed, it can be numerically demonstrated that if μ is close to -2, for a wide range values for ϵ, there exists root x_0 of $q_1^{(\beta)}$ that satisfies $0 < x_0 \ll 1$ and, therefore, the scattering can be substantially intensified. For ordinary PIM there is no such a root x_0, as can be inferred from Eq. (14). Similar case holds for electric dipole resonance when ϵ is close to -2, due to electromagnetic symmetry. In Fig. 2(a), Q_s vs x is shown for the cases with $(\epsilon, \mu) = (-2.1, -1)$ and $(-10, -1.9)$. The scattering enhancement near the electric and magnetic dipole resonances is clearly seen at $x \approx 0.234$ and 0.219, respectively, which are roots of $q_1^{(\alpha)}$ and $q_1^{(\beta)}$, respectively. Also shown in Fig. 2(a) is Q_s vs x for the case with $\epsilon = 10$ and $\mu = 2$, typical for ordinary PIM. No resonance arises at $x \ll 1$ (although resonance exhibits in intermediate regime), resulting in a much smaller Q_s when $x \ll 1$.

The enhancement of scattering due to the unusual resonance in NIM possesses some unique properties which distinguishes itself from that originating from the ordinary resonance in PIM. The ordinary resonance cannot arise in the long wavelength limit. As a result, for $x \to 0$ the scattering is always governed by Rayleigh law ($Q_s \propto x^4$). Thus one cannot enhance localization tendencies by reducing x. The un-
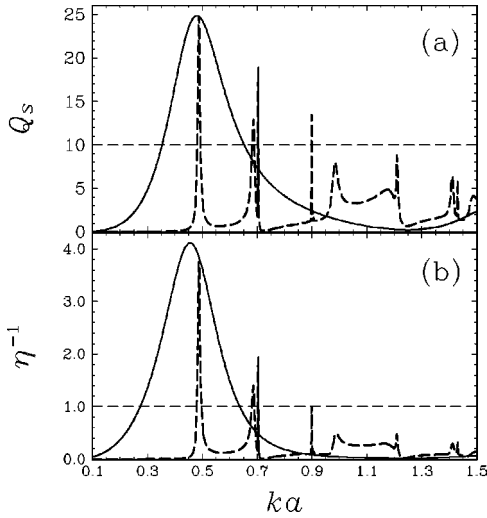
FIG. 3. The efficiency for scattering Q_s (a) and the inverse of the localization parameter η^{-1} (b) vs size parameter ka for the cases with $\epsilon=-5.5$, $\mu=-1.8$ (solid line) and $\epsilon=40$, $\mu=1$ (dashed line).

usual resonance for NIM occurs at $x \to 0$, and it greatly enhances the scattering in the Rayleigh limit, as has been demonstrated in Fig. 2. In addition, for the usual resonances in PIM, Q_s decreases rapidly as x moves away from the resonance point, thus the scattering enhancement is sensitive to the size parameter. This adds considerably to the difficulty in achieving efficient light scattering to induce localization. The enhancement due to the unusual resonance in NIM appears more robust and is insensitive to the size parameter x. This unique property is manifested clearly in Fig. 3(a), where Q_s is plotted as a function of x for the cases with $\epsilon=-5.5$, $\mu=-1.8$ and $\epsilon=40$, $\mu=1$. The material parameters ϵ and μ are so selected that the peak position and magnitude of Q_s for both cases are roughly the same, which arises at $x \sim 0.485$ with $Q_s \sim 25$. It is clearly seen that the enhancement of Q_s for NIM is more robust and less sensitive to x as compared with that for ordinary PIM. For the cases as shown in Fig. 3(a), $Q_s > 10$ when $0.35 < x < 0.65$ for the NIM, while $Q_s > 10$ is limited to a far smaller range of x, $0.48 < x < 0.49$, for the PIM.

III. EFFECT OF DISPERSION

All NIM's that have been made [5–8,11–13], with both negative ϵ and negative μ, are dispersive. The negative μ and ϵ originate from resonance, with their magnitudes varying continuously from zero to a very negative value in the frequency range of negative refractive index. As a result, with dispersive NIM particles, one can always find a frequency range such that μ or ϵ is close to -2. This feature, together with the characteristic that the scattering enhancement at low frequency is insensitive to the size of scatterers when μ or ϵ is close to -2, implies that one does not have to do anything special to achieve scattering enhancement (provided that the particles can be made sufficiently small), the scattering will be intensified for some particular frequency. We give in Fig. 4(b) numerical results of Q_s for dispersive
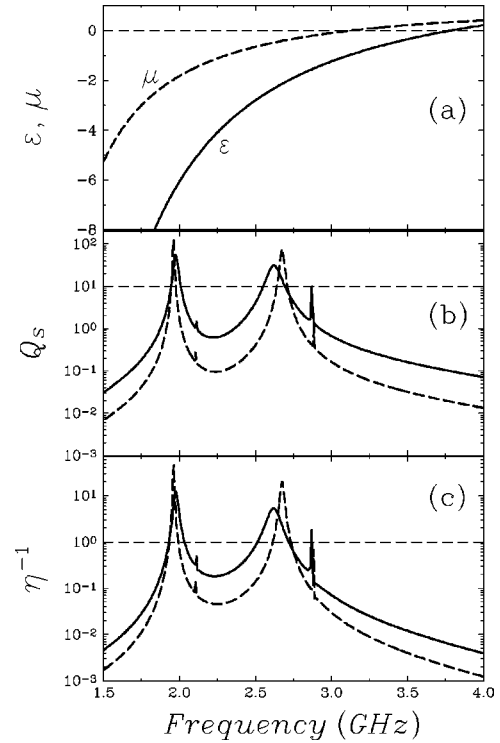

FIG. 4. (a) ϵ and μ of the NIM as given by Eqs. (22) and (23); (b) The efficiency for scattering Q_s vs frequency with material parameters as shown in (a) and radius of scatterer $a=0.8$ cm (solid line) and 0.5 cm (dashed line); (c) The inverse of the localization parameter η^{-1} vs frequency with material parameters as shown in (a) and $a=0.8$ cm (solid line) and 0.5 cm (dashed line).

NIM particle, with effective $\epsilon_s(f)$ and $\mu_s(f)$ assuming the most frequently adopted form [9],

$$\epsilon_s(f) = 1 + \frac{5^2}{0.9^2 - f^2} + \frac{10^2}{11.5^2 - f^2}, \qquad (22)$$

$$\mu_s(f) = 1 + \frac{3^2}{0.902^2 - f^2}, \qquad (23)$$

where f is the frequency in units of GHz. The dispersion forms (22) and (23) have been adopted for numerical calculation of one-dimensional photonic band of layered heterostructures combining PIM's and NIM's [9], where an unconventional type of stop bands was established. Numerical values of $\epsilon_s(f)$ and $\mu_s(f)$ are given in Fig. 4(a) in the frequency range of negative refractive index. The efficiency for scattering Q_s is shown in Fig. 4(b). Q_s clearly shows two dominant peaks at ϵ and μ close to -2, respectively, corresponding to the cases near the electric and magnetic dipole resonances, respectively. Two small peaks appear at ϵ and μ close to $-3/2$, corresponding to the electric and magnetic quadrupole resonances. In particular, in Fig. 4(b) it can be seen that the frequency regime where the scattering is greatly enhanced is nearly unchanged even if the radius of the NIM sphere changes from 0.8 cm to 0.5 cm, demonstrating the unique property that the enhancement of scattering is insen-

sitive to the size of the scatterers. This robustness is expected to help clearing up some difficulties in the experimental realization of light localization.

IV. LOCALIZATION

Using the results of the scattering from a single sphere, we numerically calculate the localization parameter η in disordered system composed of NIM particles with typical volume fraction $f_v = 10\%$ based on Eq. (1). Figures 2(b) and 3(b) show η^{-1} vs x, while in Fig. 4(c) the dependence of η^{-1} on frequency is given for more realistic dispersive NIM's. Figure 2(b) suggests that a much smaller η can be achieved with the use of NIM's that both increase Q_s and shift the strong scattering regime to the small-particle limit. From Fig. 3(b), it is found that the reduction of η is more robust and insensitive to the size of the scatterers as compared with the ordinary PIM's, similar to the results for Q_s. It is seen from Fig. 4(c) that the magnitude of η can be reduced to 10^{-2}, demonstrating a possibility of realizing light localization using randomly distributed NIM scatterers in practice.

The great enhancement of scattering for NIM's due to the characteristic $x \to 0$ resonant behavior in the small-particle limit may introduce an extra time delay in light propagation, causing a considerable decrease of v_E, the energy transport velocity, in comparison with the ordinary case. The diffusion constant $D = (1/3)v_E l_t$ may also be strongly affected, not only through l_t but also through v_E, due to $x \to 0$ resonance in the presence of NIM's. By taking advantage of the $x \to 0$ resonance unique in NIM's, many unusual electromagnetic transport properties in random media may be explored.

V. CONCLUSION

In summary, we have studied the influence of NIM scatterers on the scattering of light and their implications in the localization parameter. An unusual resonant behavior is found at $ka \to 0$, which leads, in small-ka limit, to a great enhancement of scattering that is insensitive to the size of scatterers. This gives rise to a significant reduction of the localization parameter. With the use of NIM's, the light localization transition may be achieved by reducing the wave vector k in analogy to electronic systems. The negative permittivity and permeability usually originate from resonance. The underlying physics for the unusual scattering behavior of the spherical NIM is thus believed to arise from the coupling between the resonance intrinsic to the NIM and the resonance due to the (nearly) self-sustained modes in spherical geometry [30]. As such, NIM particles of other geometry may share the similar unusual enhancement of scattering in the small-particle limit [32]. Besides the light localization, the phenomenon is expected to find many other applications as well, in particular, in devices exploring the transport properties of electromagnetic waves through random media.

Note added. After the submission of this manuscript, we learned that an analogous work with two-dimensional cylindrical structures has been done by Alù and Engheta [32].

[1] R. Fitzgerald, Phys. Today **53**, 17 (2000); M.C.K. Wiltshire, Science **292**, 5514 (2001).

[2] J.B. Pendry, A.J. Holden, W.J. Stewart, and I. Youngs, Phys. Rev. Lett. **76**, 4773 (1996).

[3] J.B. Pendry *et al.*, IEEE Trans. Microwave Theory Tech. **47**, 2075 (1999).

[4] J.B. Pendry, Phys. Rev. Lett. **85**, 3966 (2000).

[5] D.R. Smith, W.J. Padilla, D.C. Vier, S.C. Nemat-Nasser, and S. Schultz, Phys. Rev. Lett. **84**, 4184 (2000).

[6] D.R. Smith and N. Kroll, Phys. Rev. Lett. **85**, 2933 (2000).

[7] R.A. Shelby, D.R. Smith, S.C. Nemet-Nasser, and S. Schultz, Appl. Phys. Lett. **78**, 489 (2001).

[8] R.A. Shelby, D.R. Smith, and S. Schultz, Science **292**, 77 (2001).

[9] J. Li, L. Zhou, C.T. Chan, and P. Sheng, Phys. Rev. Lett. **90**, 083901 (2003).

[10] D.R. Smith and D. Schurig, Phys. Rev. Lett. **90**, 077405 (2003).

[11] C.G. Parazzoli, R.B. Greegor, K. Li, B.E.C. Koltenbah, and M. Tanielian, Phys. Rev. Lett. **90**, 107401 (2003).

[12] S. Foteinopoulou, E.N. Economou, and C.M. Soukoulis, Phys. Rev. Lett. **90**, 107402 (2003).

[13] A.A. Houck, J.B. Brock, and I.L. Chuang, Phys. Rev. Lett. **90**, 137401 (2003).

[14] J.B. Pendry, Opt. Express **11**, 639 (2003).

[15] V.G. Veselago Sov. Phys. Usp. **10**, 509 (1968).

[16] Z.M. Zhang, C.J. Fu, Appl. Phys. Lett. **80**, 1097 (2002).

[17] Z. Liu, L.B. Hu, and Z.F. Lin, Phys. Lett. A **308**, 294 (2003).

[18] Y. Kuga and A. Ishimaru, J. Opt. Soc. Am. A **8**, 831 (1984).

[19] M.P. Van Albada and A. Lagendijk, Phys. Rev. Lett. **55**, 2692 (1985).

[20] P.E. Wolf and G. Maret, Phys. Rev. Lett. **55**, 2696 (1985).

[21] I. Freund, M. Rosenbluh, and S. Feng, Phys. Rev. Lett. **61**, 2328 (1988).

[22] N. Garcia and A.Z. Genack, Phys. Rev. Lett. **63**, 1678 (1989); **66**, 1850 (1991).

[23] M.P. van Albada, J.F. de Boer, and A. Lagendijk, Phys. Rev. Lett. **64**, 2787 (1989).

[24] G.L.J.A. Rikken and B.A. van Tiggelen, Nature (London) **381**, 54 (1996).

[25] B.A. van Tiggelen *et al.*, Phys. Rev. Lett. **77**, 639 (1996); H. Stark and T.C. Lubensky, *ibid.* **77**, 2229 (1996).

[26] D.S. Wiersma, P. Bartolini, A. Lagendijk, and R. Righini, Nature (London) **390**, 671 (1997).

[27] F. Scheffold *et al.*, Phys. Rev. Lett. **81**, 5800 (1998); Nature (London) **398**, 206 (1999).

[28] C. M. Soukoulis, *Photonic Crystals and Light Localization in*

the 21st Century (Kluwer Academic, Dordrecht, 2001).

[29] C. F. Bohren and D. R. Huffman, *Absorption and Scattering of Light by Small Particles* (Wiley, New York, 1983).

[30] H. C. van de Hulst, *Light Scattering by Small Particles* (Dover, New York, 1981).

[31] R. Ruppin, Solid State Commun. **116**, 411 (2000).

[32] A. Alù and N. Engheta, in Proceedings of the International Conference on Electromagnetics in Advanced Applications, ICEAA 03, Torino, Italy, 2003 (unpublished).